A Model for the Dynamics of Space

- Expedition to the Early Universe -

Hans-Otto Carmesin*

*Gymnasium Athenaeum Stade, Harsefelder Straße 40, 21680 Stade, Studienseminar Stade, Bahnhofstraße 5, 21682 Stade, Fachbereich Physik, Universität Bremen, 28334 Bremen
Hans-Otto.Carmesin@t-online.de

Abstract

The expansion of our universe is fascinating. Additionally there are exciting mysteries about the early universe: How is causality achieved? Why is quantum gravity essential? How can the problems of reheating and big bang singularity be solved? Here I present a teaching unit that I developed and tested in a research club at school. The 'process related competences' of 'modeling' and 'problem solving' are applied: Observations are modeled systematically. Problems are utilized to improve the models progressively. Additionally models developed by the teacher are available for critical tests and cooperative research projects.

1. Introduction

The formation of models by students is an essential topic at school (Kultusministerium, 2017). Accordingly we start with observational data about the expanding and about the early universe and we form corresponding models. Thereby we start with simple models and improve these when necessary. In order to improve a model we establish a cognitive conflict first. This conflict establishes a problem to be solved by the students with help of the teacher. Such problem solving establishes a particularly efficient method for learning (Hattie, 2009). As a result we develop a progressive sequence of models, all related to observations and solving problems that are inherent to the previous model. In that process a model first establishes a hypothesis about a solution of a problem and this hypothesis is critically tested by the students themselves. Such a learning by forming hypotheses and testing these actively is a particularly efficient method for learning (Hattie, 2009). Altogether I present a teaching unit about the early universe. Additionally I report about experiences with teaching this sequence in a research club at school. The students are from classes 9 to 12. Each of the following sections describes the content of a lesson. Thereby the activity of the students is emphasized by italic letters. Performing research in a research club one might arrive at a novel theory. This is presented at the end of this report.

2. Discovery of the Hubble law

The students observed distant galaxies with help of our school observatory (Carmesin, 2012). They determined the redshifts z and they either estimated the distance similarly as Carl Wirtz did it (Wirtz, 1922) or they applied data about the distance d from the literature (see figure 1). As a result we obtain the Hubble law $d \sim z$ (Hubble, 1929). The proportionality factor z/d is named Hubble constant H_0.

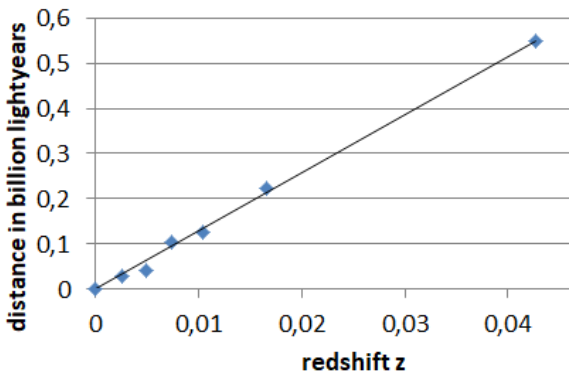

Figure 1: Hubble diagram: redshifts observed by students at the school observatory using a telescope with the aperture 11'' (Helmcke u. a. 2018).

3. First model: discovery of age of our universe

In order to develop a first model for the observed Hubble law, the students model a radial velocity v for distant galaxies. Corresponding lessons are presented in Carmesin (2014). Thereby we apply the Doppler effect to the emitted wavelength $\lambda_e = c \cdot T$ and obtain the observed wavelength λ_{obs} as follows:

$$\lambda_{obs} = \lambda_e + v \cdot T \qquad \{1\}$$

We solve for the velocity and obtain:

$$v = c \cdot z \quad \text{with} \quad z = (\lambda_{obs} - \lambda_e)/\lambda_e \qquad \{2\}$$

So we obtain a radial velocity v for each galaxy and we can determine from our data when the distance d of that galaxy was zero. Here we discover that the distance was zero 14 billion years ago for each distant galaxy. This establishes our first concept of the big bang.

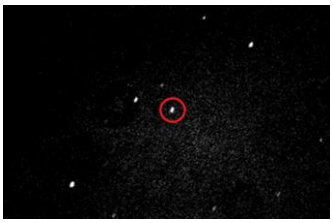

Figure 2: Quasar APM 8279+5255 at redshift z = 3.9 observed by students at the school observatory using a telescope with the aperture 11''.

4. Observation of a very distant quasar

In our school observatory our students observed very distant galaxies or quasars and took pictures. For instance they made a picture of the quasar APM 8279+5255 (see figure 2). That quasar has the redshift z = 3.9. According to equation {2} the velocity would take the value v = 3.9c. This contradicts other observations of our students according to which the velocity of an object in space cannot exceed the velocity of light c (Carmesin, 2006). So the student's own observations give rise to a **cognitive conflict** or a falsification of our first model at large z (Popper 1974). Accordingly our task or problem is to establish an improved model.

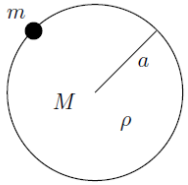

Figure 3: Second model: Prototypical ball of the universe with a radius a, volume V, density ρ mass $M = \rho \cdot V$ and a small probing mass m. In the early universe the mass is present in terms of the equivalent energy $E = M \cdot c^2$ or $E = m \cdot c^2$.

5. Second model: expansion of space

The Hubble law or the increase of the redshift z proportional to the distance d might be explained by an expansion of space. Next we test this hypothesis. *For it the students perform a model experiment*: they draw a wave onto a balloon and measure how it grows with increasing radius. The result is in rough accordance with the Hubble law.

Progressively the students develop a dynamical model that provides the fully relativistic Friedmann – Lemaitre equation FLE (Friedmann, 1922; Lemaitre, 1927; Unsöld, 1999). From a didactic point of view they apply the hypothetic deductive method (Kircher, 2001). For it we model a mass m on a sphere with radius a and mass M (see figure 3).

6. Rate of expansion

With the model (see figure 3) the students analyze the dynamics in a next lesson. *The students establish the energy equation of the probing mass*:

$$E = \tfrac{1}{2} \cdot m \cdot v^2 - G \cdot M \cdot m/a \qquad \{3\}$$

In the framework of the first model and the Hubble constant H_0 the students realize that the rate v/a is essential since it corresponds to H_0. More generally this rate may vary with time and is named Hubble parameter H correspondingly:

$$H = v/a \qquad \{4\}$$

Accordingly equation {3} is solved for the Hubble parameter:

$$H^2 = 8\pi G \cdot \rho/3 - k \cdot c^2/a^2 \qquad \{5\}$$

Thereby we abbreviate the scaled mechanical energy $-2E/(m \cdot c^2)$ by a parameter k. *Altogether the students derive the dynamics* (equation {5}) with little help. That dynamics presents the well - established Friedmann Lemaitre equation FLE (Unsöld, 1999). *Here the students discover that the rate of expansion H is not fixed like in figure 1, but it increases with the density. Moreover that rate H depends on the scaled mechanical energy k.*

That scaled energy k is interpreted further as follows: Some students know already that k additionally describes the curvature of space and that it is approximately zero (Carmesin, 2014). While the full analysis is presented in (Carmesin, 2018a) we consider k = 0 here, since it corresponds to observations (Planck Collaboration 2016).

7. Discovery of the big bang singularity

In this lesson the students perform a computer simulation with equation {5} which establishes a differential equation. With it the students determine the time development of the radius a(t) with a computer simulation based on the Euler method. When they investigate the radius a(t) for the past then they observe that the radius a(t) tends to zero. Correspondingly the density ρ tends to infinity. A diverging density is not realistic. It is named the big bang singularity (Kiefer, 2008). *With it the students experience the next **cognitive conflict** and falsify our second model as well as the Friedmann Lemaitre equation at large density*. So we look forward to develop a model for very high densities. For it we develop a model for a white dwarf first.

8. A model for a white dwarf

In this lesson the students model a white dwarf in order to investigate states at high density (Sexl, 1975). For it the students apply their knowledge about quantum physics to a white dwarf. In such a star the electrons move freely at high density. *The students realize that the required space is limited by the Heisenberg uncertainty relation*, including the Planck constant h as well as the reduced Planck constant $\underline{h} = h/(2\pi)$ (Ballentine, 1998):

$$\Delta p \cdot \Delta x \geq \tfrac{1}{2} \cdot \underline{h} \qquad \{6\}$$

The students model the wave function as follows. It is plausible that the extension of electrons at high density might be modeled by Gaussian wave packets ψ. Correspondingly the students learned some basics about Gaussian wave packets in an extra lesson

about mathematical tools. In particular we may replace the inequality in equation {6} by the equality for the case of such wave packets. Moreover we apply the momentum of the relativistic electron $p = m \cdot c \geq \Delta p$. Accordingly we get:

$$\Delta x = \tfrac{1}{2} \cdot \underline{h}/(mc) = 0.19 \text{ pm} \qquad \{7\}$$

The students calculate the density as follows: We consider one proton per electron. Thereby the proton mass is $m_{Pr} = 1.67 \cdot 10^{-27}$ kg. So we obtain:

$$\rho = m_{Pr}/(4\pi/3 \cdot \Delta x^3) = 58 \cdot 10^9 \text{ kg/m}^3 \qquad \{8\}$$

The students test their model by comparison with the white dwarf Sirius B with the mass $M = 2 \cdot 10^{30}$ kg, the radius 6000 km and density $\rho = 2.2 \cdot 10^9$ kg/m^3. So our very simple model is in rough accordance with observations.

The students investigate the stability of the white dwarf as follows. The gravitational energy causes an inward pressure p_{in} while the kinetic energy of the electrons causes an outward pressure p_{out}. So we compare these two pressures.

The pressure is the derivative of the energy E as a function of volume V:

$p=E(V)'=E(R)'\cdot R(V)'=E(R)'/V(R)'=E(R)'/(4\pi R^2)$

The gravitational energy is $E_{pot} \approx - G \cdot M^2/R$, accordingly we get:

$$p_{in} \approx G \cdot M^2/(4\pi R^4) \qquad \{9\}$$

The kinetic energy of an electron is $E = p \cdot c$ or $E \approx \tfrac{1}{2} \cdot \underline{h} \cdot c/\Delta x$. Moreover the extensions R of the star and Δx of the electron are related by $\Delta x = R/N^{1/3}$. Furthermore the number of electrons is $N = M/m_{Pr}$. Accordingly we get

$$p_{out} = \tfrac{1}{2} \cdot \underline{h} \cdot c \cdot N^{4/3} / (4\pi R^4) \qquad \{10\}$$

The instability occurs when both pressures are equal:

$$G \cdot M^2 = \tfrac{1}{2} \cdot \underline{h} \cdot c \cdot M^{4/3} m_{Pr}^{-4/3} \qquad \{11\}$$

We solve for this critical mass:

$$M_{cr} = (\tfrac{1}{2} \cdot \underline{h} \cdot c/G)^{3/2} m_{Pr}^{-2} = 1.3 \cdot 10^{30} \text{ kg} \qquad \{12\}$$

Altogether the students discover the gravitational collapse at that critical mass of the white dwarf (Chandrasekhar, 1931). As a consequence the white dwarf may become a neutron star. At the example of the white dwarf and its gravitational instability the students obtained sufficient experience and curiosity in order to investigate the big bang singularity next.

9. Planck scale: static limitation of density

In this lesson the students realize that two basic physical effects limit the states that can be measured at all: The Heisenberg uncertainty principle (equation {6}) as well as gravity with its Schwarzschild radius:

$$\Delta x \geq R_S = 2G \cdot M/c^2 \qquad \{13\}$$

The students combine these two limitations in a distance energy diagram. For it they express the limitations in terms of energies depending on the observable distance $r = \Delta x$:

$$r \geq 2G \cdot E/c^4 \quad \text{and} \quad r \geq \tfrac{1}{2} \cdot \underline{h} \cdot c/E \qquad \{14\}$$

These conditions are combined graphically in figure 4: the solid line and the solid ruled area present conceivable measurements according to gravity while the dashed line and the dashed ruled area present conceivable measurements according to quantum physics. The area ruled by dashed as well as solid lines presents conceivable physical measurements. The other areas do not present any conceivable physical measurements at all.

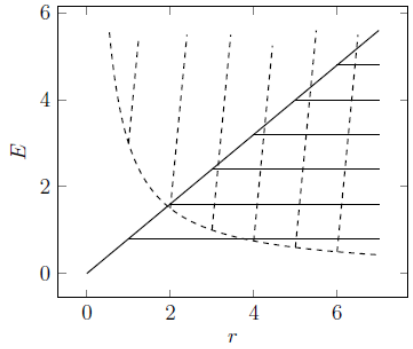

Figure 4: Planck scale

The students discover the smallest measurable length L_P at the intersection point of the solid and dashed line. It is called Planck (1899) length:

$$L_P = (\underline{h} \cdot G/c^3)^{0.5} = 1.616 \cdot 10^{-35} \text{ m} \qquad \{15\}$$

The corresponding density sets an upper limit for the density (Carmesin, 2017, 2018a) and is named Planck density:

$$\rho_P = c^5 / (\underline{h} \cdot G^2) = 5.155 \cdot 10^{96} \text{ kg/m}^3 \qquad \{16\}$$

So the students discover the static limitation of the density from first principles: gravity and quantum physics. Correspondingly that limitation is expressed by the fundamental physical constants G, c and h. This establishes an essential result of quantum gravity that the students discover in the present teaching unit. The students asked the naturally next question: how is that static limitation achieved dynamically? This is investigated in the following lesson.

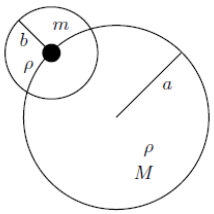

Figure 5: Third model: Probing mass with radius b.

10. Third model: regular probing mass

In this lesson the students realize the singular nature of the point like probing mass in figure (3). Accordingly they generalize that probing mass by a ball (figure 5). Correspondingly we improve the second model by including a radius b of the probing mass m. This is in accordance with the cosmological principle: homogeneous density and isotropy.

According to the Heisenberg uncertainty relation the energy of the probing mass (see equation {3}) is expressed in terms of the momentum:

$$E = ½ \cdot p^2/m - G \cdot M \cdot m/a \qquad \{17\}$$

The students ask: how are the radius b and the mass m determined at a density ρ? *The students realize that the mass depends on the radius* $m = \rho \cdot b^3 \cdot 4\pi/3$. So only the determination of b or m is difficult. *At this point we must realize that we work with a novel model and that we must develop tools in order to gain results. For it the students are reminded to the typical minimization of energy in nature. For instance a ball typically rolls downwards*. They are told that the corresponding states are named ground states and that the procedure of minimization is called variational principle in quantum mechanics. According to the law of energy conservation, the determination of the optimal mass corresponds to a fragmentation of mass or equivalent energy inherent to the density ρ into probing masses m. For it the energy E per mass is minimized in the following. Accordingly we divide the above equation by $m \cdot c^2$:

$$E/(m \cdot c^2) = ½ \cdot p^2/(m^2 \cdot c^2) - G \cdot M/(a \cdot c^2) \qquad \{18\}$$

Next the students determine the expectation value < … >. For it they apply their knowledge that the probability density $|\psi|^2$ corresponds to the wave function ψ (Kultusministerium, 2017). For short we denote the expectation value of the scaled energy by $<E/(m \cdot c^2)> = E_{D,full}$. Accordingly we get:

$$E_{D,full} = ½ \cdot <p^2/(m^2 \cdot c^2)> - G \cdot <M/(a \cdot c^2)> \qquad \{19\}$$

The students realize that two quantities should be varied at a given density ρ: the probing mass m as well as the width Δa of the Gaussian.

For it they mark the states with a given density ρ by a dotted line in figure 6. *The students realize graphically how the optimum is achieved*: the scaled energy $E_{D,full}$ in equation {19} is minimal at maximal m. Thereby m is restricted to the dotted line and to the double ruled area in figure 6. Consequently m corresponds to the intersection point of the solid and dotted line in figure 6. As a result m corresponds to the Schwarzschild radius at the given density ρ:

$$b = 2G \cdot m/c^2 \qquad \{20\}$$

The students simplify this equation by introducing further Planck units (Planck, 1899):

$$M_P = L_P^3 \cdot \rho_P \quad \text{and}$$

$$\underline{\rho}_P = \rho_P/(4\pi/3) = 1.231 \cdot 10^{96}\ kg/m^3 \qquad \{21\}$$

As a consequence we get:

$$M_P = \underline{h}/(L_P \cdot c) \qquad \{22\}$$

We introduce scaled variables and denote these by bold letters:

$$\mathbf{m} = m/M_P;\ \mathbf{b} = b/L_P;\ \boldsymbol{\rho} = \rho/\underline{\rho}_P \qquad \{23\}$$

With these formulas the students transform equation {20} into:

$$\mathbf{b}^{-2} = 2 \cdot \boldsymbol{\rho} \quad \text{or} \quad \mathbf{m}^{-2} = 8 \cdot \boldsymbol{\rho} \qquad \{24\}$$

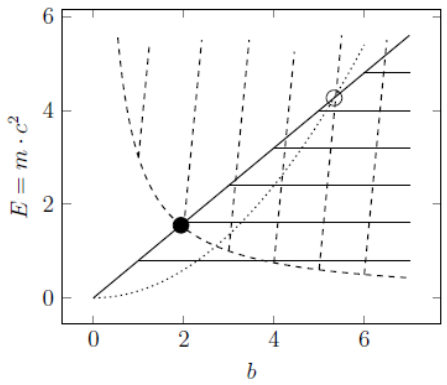

Figure 6: Fragmentation or partitioning into probing masses m: Dotted line: constant density.

Altogether the students discover the optimal probing mass with little help as follows: the minimization of the scaled energy $E_{D,full}$ causes a fragmentation or partitioning into particular probing masses with particular and regular extension b. Note that these balls cannot fill the complete space for geometric reasons and that this is confirmed by an application of the present model to the emergence of dark matter (Carmesin, 2018a). At this point the students are familiar with the variational principle and they apply it to the width Δa of the Gaussian wave packets ψ in the following lesson.

11. Regular dynamics

The students apply the variational principle to the Gaussian wave packets with some help as follows. They apply the mathematical identity $<p^2> = <p>^2 + (\Delta p)^2$ to equation {19} and neglect <p> here, since <p> forms according to the FLE in a slow dynamics while the wave function ψ forms in a rapid dynamics:

$$E_D = ½ \cdot \Delta p^2/(m^2 \cdot c^2) - G/c^2 \cdot <M/a> \quad \text{and}$$

$$E_{D,full} = E_D + ½\ p^2/(m^2 \cdot c^2) \qquad \{25\}$$

Thereby we denote <p> shortly by p in the following. Here the Heisenberg uncertainty principle in three dimensions is applied for Gaussian wave packets:

$$\Delta p = ½ \cdot 3\ \underline{h}/\Delta a \qquad \{26\}$$

Accordingly we get:

$$E_D = 9\underline{h}^2/(8 \cdot m^2 \cdot c^2 \cdot \Delta a^2) - G/c^2 \cdot <M/a> \qquad \{27\}$$

Classically, the radius a(t) describing the space of the sphere in figure (5) can be chosen arbitrarily. However, here that space is primarily filled by radiation. Accordingly we choose the radius a(t) corresponding to a photon starting at the Planck density and expanding according to the expansion of space. For additional background see Carmesin (2018a). Such a photon is characterized by the dashed line in figure 6 and by the term:

$$M = M_P \cdot L_P/a \qquad \{28\}$$

The students learned in the additional lesson about mathematical tools how to generate a linear approximation including a statistical approximation and

verified these approximations numerically. *Accordingly the students simplify the gravitational term with some help as follows*:

$$\langle M/a\rangle = M_P \cdot L_P \cdot \langle 1/a^2\rangle \approx M_P \cdot L_P \cdot 1/\langle a^2\rangle$$
$$= 1/(\langle a\rangle^2 + \Delta a^2) = 1/\langle a\rangle^2 \cdot 1/(1+[\Delta a/\langle a\rangle]^2)$$
$$\approx 1/\langle a\rangle^2 \cdot (1 - [\Delta a/\langle a\rangle]^2) \quad \{29\}$$

In the following we apply the abbreviation $a = \langle a\rangle$. Accordingly we express the scaled energy E_D in terms of the classical term $E_{D,cl}$ and the quantum term $E_{D,Q}$ as follows:

$$E_D = E_{D,cl} + E_{D,Q} \quad \text{with}$$
$$E_{D,cl} = -G\cdot M/(c^2\cdot a) \quad \text{and}$$
$$E_{D,Q} = 9\underline{h}^2/(8m^2\cdot c^2\cdot \Delta a^2) + G\cdot M\Delta a^2/(c^2\cdot a^3) \quad \{30\}$$

The students scale the terms (see equations {21}-{24}) as follows:

$$E_{D,cl} = -\boldsymbol{\rho}\cdot \mathbf{a}^2 \quad \{31\}$$
$$E_{D,Q} = 9\cdot \boldsymbol{\rho}\cdot (\Delta \mathbf{a})^{-2} + \boldsymbol{\rho}\cdot (\Delta \mathbf{a})^2 \quad \{32\}$$

The students minimize the quantum term $E_{D,Q}$ by variation of $\Delta \boldsymbol{a}$ and obtain:

$$\Delta \mathbf{a} = 3^{0.5} \quad \text{and} \quad E_D = -\boldsymbol{\rho}\cdot \mathbf{a}^2 + 6\,\boldsymbol{\rho} \quad \{33\}$$

The students express E_D by the density. For it they apply equation {28}:

$$\boldsymbol{\rho} = M/a^3 \cdot L_P{}^3/M_P = M_P L_P/a^4 \cdot L_P{}^3/M_P = \mathbf{a}^{-4} \{34\}$$

They apply this relation to equation {33} and obtain:

$$E_D = -\boldsymbol{\rho}^{1/2} + 6\,\boldsymbol{\rho} \quad \{35\}$$

Next the students generalize the FLE {5} by application of the term E_D. For it we remind equation {25}:

$$E_{D,full} = E_D + \tfrac{1}{2}\, p^2/(m^2\cdot c^2)$$

Thereby we remind that $E_{D,full}$ is proportional to the curvature parameter k. We consider the case k = 0. Moreover we insert $p = m\cdot v$ and solve for $H^2 = v^2/a^2$:

$$H^2 = -\ 2E_D \cdot c^2/a^2 \quad \{36\}$$

The students introduce scaled variables. For it we apply the Planck time:

$$t_P = L_P \cdot c = 5.391\cdot 10^{-44}\ \text{s} \quad \{37\}$$

We introduce the scaled Hubble parameter by multiplication with t_P and get:

$$\mathbf{H} = H \cdot t_P \quad \{38\}$$

Accordingly we express the dynamics in equation {36} as follows:

$$\mathbf{H}^2 = -\ 2E_D/\mathbf{a}^2 = -\ 2E_D \cdot \boldsymbol{\rho}^{1/2} \quad \{39\}$$

Here we insert the term for E_D (see equation {35}) and factorize **ρ**:

$$\mathbf{H}^2 = 2\cdot \boldsymbol{\rho}\cdot (1 - 6\cdot \boldsymbol{\rho}^{1/2}) \quad \{40\}$$

This equation is an extended FLE, denoted by EFLE. With H = v/a it is a differential equation and establishes the dynamics. Here the students analyze that the dynamics stops when the bracket becomes zero at $\boldsymbol{\rho}_{max} = 1/36$. Accordingly the density cannot become larger than the Planck density. *Altogether the students exclude the big bang singularity*. A similar maximal density has been obtained by Bojowald (2001).

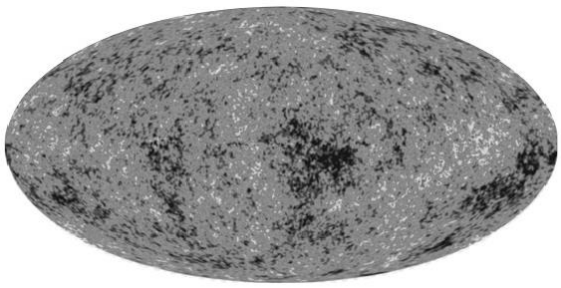

Figure 7: Cosmic microwave background CMB (figure: NASA WMAP Science Team, 9 year WMAP image of background radiation: The temperature fluctuations are very small $\Delta T/T = 0.000024$.

12. CMB: horizon problem

The energy fluctuations of the early universe are very small (see figure 7). So energy fluctuations must have been compensated by mutual exchange of radiation among regions of the CMB. However, with the dynamics of the FLE or of the EFLE that is impossible as shown by Alan Guth (1981). This is called the horizon problem. Moreover Alan Guth suggested that the early universe expanded very rapidly by a factor $Z = e^N$ with $55 \le N \le 70$ (Guth, 1981 or Broy, 2016). However there is not sufficient energy in the universe for such an expansion. This is named the reheating problem (Broy, 2016 or Carmesin, 2018a). Here we study whether the model in figure (5) shows how the required enlargement occurs as a result of gravity and quantum physics.

For it we consider a situation at the Planck density. Regions with mass or equivalent energy strongly attract each other, but the distances cannot decrease any further.

This is a severe problem for gravity. Usually gravity always finds a way to compress things. How can gravity compress things at the Planck density? Here we remind that space has a grainy nature at least near the Planck density. And grains are usually connected to three dimensional space. So gravity might reorganize the dimension in order to compress things further. Is this possible? *In order to answer this question the students perform a model experiment with magnetic balls (see figure 8)*. Thereby they discover that a decrease of dimension causes an enlargement (see figure 8). *So the students realize that gravity at high density might cause another gravitational instability: the collapse to higher dimension and conversely decreasing density might cause the unfolding of space by decreasing dimension D*. Accordingly the students look forward to calculate the critical density for such a gravitational collapse of dimension.

13. Fourth model: variable dimension

In this lesson the students generalize the third model (see figure 3) to dynamical dimension. For it the Gauss law of gravitation (Gauss, 1813) is presented and the energy of the probing mass (equation {18})

is generalized accordingly to arbitrary dimension D ≥3 (for details see Carmesin 2017, 2018a):

$E/(m\cdot c^2)=½\cdot p^2/(m^2\cdot c^2) - G_D\cdot M/(a^{D-2}\cdot c^2\cdot[D-2])$ {41}

Thereby the gravitational constant G_D is:

$G_D = G\cdot(D-2)\cdot L_p^{D-3}$ {42}

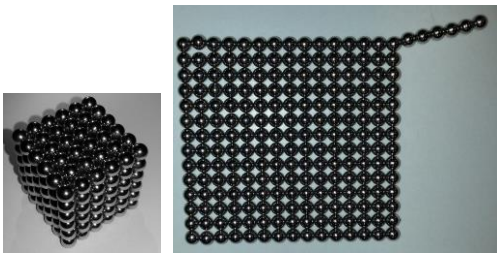

Figure 8: 216 magnetic balls organized in three dimensions (left). When the dimension decreases then the distances increase (right).

Moreover we denote the volume of the ball in D dimensions with radius 1 by V_D and we define the density corresponding to Dimension D as follows:

$\rho_D = M \cdot V_D^{-1} \cdot a^{-D}$ {43}

At this point the students realize that the model is solved in D dimensions by the same procedure as at D = 3. So they solve the model with little help as follows.

The students derive a term for the Schwarzschild radius from equation {41}:

$½\ m\cdot c^2 = G_D\cdot M\cdot m/(R_{SD}^{D-2}\cdot[D-2])$ or {44}

$\mathbf{R}_{SD}^{-2} = 2\ \boldsymbol{\rho_D}$ {45}

Next the students determine the scaled optimal radius (see figure 6):

$R_{SD} = b$ or $\mathbf{b}^{-2} = 2\cdot \boldsymbol{\rho_D}$ {46}

From it the students determine the scaled optimal probing mass:

$\mathbf{m} = 2^{-D/2} \cdot \boldsymbol{\rho_D}^{(2-D)/2}$ {47}

Analogously as for D = 3 the students express the radius a in terms of the density:

$\mathbf{a}^{D+1} = 1/\boldsymbol{\rho_D}$ {48}

With the above results the students determine the scaled energy E_D and obtain:

$E_D = E_{D,cl} + E_{D,Q}$ with $E_{D,cl} = -\boldsymbol{\rho_D}^{(D-1)/(D+1)}$ and

$E_{D,Q} = D^2\cdot 2^{D-3}\cdot \boldsymbol{\rho_D}^{D-2}/\boldsymbol{\Delta a}^2 + \boldsymbol{\rho_D}\cdot\boldsymbol{\Delta a}^2\cdot(D-1)/2$ {49}

Analogously as at D = 3 the students determine the optimal quantum fluctuations Δa by minimizing E_D. So they get:

$\boldsymbol{\Delta a} = [2^{D-2}\cdot D^2/(D-1)]^{0.25}\cdot \boldsymbol{\rho_D}^{(D-3)/4}$ and

$E_D = -\boldsymbol{\rho_D}^{(D-1)/(D+1)} + [2^{D-2}\cdot D^2\cdot(D-1)]^{0.5}\cdot \boldsymbol{\rho_D}^{(D-1)/2}$ {50}

14. Dimensional transitions at critical densities

In this lesson the students minimize the scaled energy E_D by variation of D according to the variational principle (see figure 9; Sprenger u. a. 2018). They discover gravitational instabilities at critical densities $\boldsymbol{\rho_{Dc}}$ (see arrows in figure 9). The students characterize the instabilities:

At an instability the dimension changes and thereby the scaled energy is minimized. At high density the stable dimension is high (see figure 10). The maximal density $\boldsymbol{\rho_{D,max}}$ is not reached, since the dimensional transition occurs before at lower density $\boldsymbol{\rho_{Dc}}$ (see figure 10). So the big bang singularity is solved by dimensional transitions. So the big bang singularity is not solved by a stopping of the dynamics (see equation {40}) as dimensional transitions occur first.

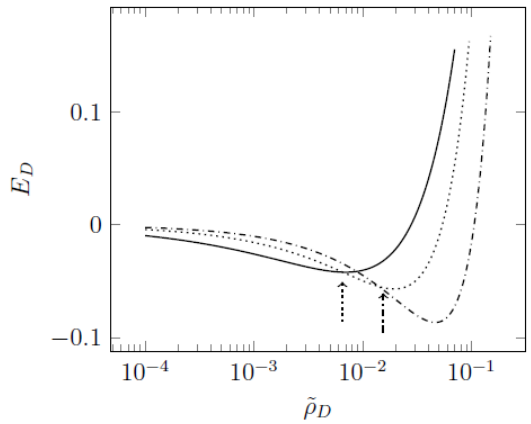

Figure 9: Scaled energy E_D at dimensions 3 (solid), 4 (dotted) and 5 (dashdotted).

In the early universe the expansion according to the FLE or EFLE causes a slight decrease of the density $\boldsymbol{\rho_D}$ and the next critical density is reached eventually, then the dimension decreases and the universe is enlarged extremely rapidly. This might explain the era of cosmic inflation.

The students planned to test this hypothesis by calculating the development of the radius r(t) of the current light horizon at the dimensional transitions and by calculating the enlargement factor $Z = e^N$. If the modeled enlargement factor Z_{model} corresponds to the observed enlargement factor with $55 \le N \le 70$ (Broy, 2016), then the model satisfies this. Note that the model satisfies many additional tests (Carmesin, 2017, 2018a,b,c,d; the flatness problem, dark matter problem and dark energy problem are solved).

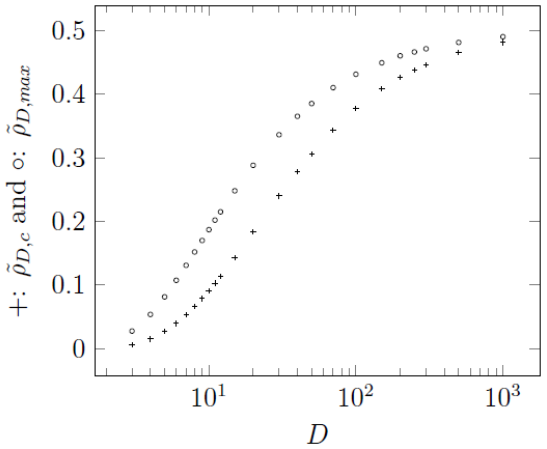

Figure 10: Scaled critical and maximal densities as a function of the dimension (Carmesin, 2018a,b).

15. Expansion of space

In this lesson the students apply the FLE in order to calculate the expansion of space backwards from the current light horizon r_{lh}.

The observable space is limited by the current light horizon r_{lh} or particle horizon and characterized by the current density of the universe ρ_{today} as well as by the current density of the matter $\rho_{today,m}$ (Planck collaboration, 2016. The density of the vacuum is not included in $\rho_{today,m}$. A more general analysis that is also independent of the current light horizon is presented in Carmesin, 2018a,b,c,d):

$r_{lh} = 4.41 \cdot 10^{26}$ m and $t_{today} = 4.35 \cdot 10^{17}$ s and

$\rho_{today} = 8.634 \cdot 10^{-27}$ kg/m^3

and $\rho_{today,m} = 2.659 \cdot 10^{-27}$ kg/m^3 {56}

Currently the density of the matter is larger than that of radiation, since the wavelength of radiation decreased according to the expansion of space (for the purpose of quantitative comparisons it is adequate to use the notion density so that it includes matter and radiation according to the equivalence $E = m \cdot c^2$). At a time t_{eq} the densities of matter and radiation were equal. The corresponding radius and density have been observed (Planck collaboration 2016):

$r_{eq} = 1.308 \cdot 10^{23}$ m and $t_{eq} = 1.55 \cdot 10^{12}$ s and

$\rho_{eq,m} = \rho_{today,m} \cdot (r_{lh}/r_{eq})^3 = 1.02 \cdot 10^{-16}$ kg/m^3 {57}

Before t_{eq} the density varied proportional to the inverse fourth power of the radius (see also equation {48}). The end of the era of cosmic inflation is marked by the critical density (see equation {52}). The corresponding radius is named r_{final} or r_f and is established as follows (see equations {21} and {52} and Unsöld, 1999):

$\rho_{3,c} = \boldsymbol{\rho_{3,c}} \cdot \varrho_P = 0.00657 \cdot 1.231 \cdot 10^{96}$ kg/m^3 $= 8 \cdot 10^{93}$ kg/m^3

and $r_f = r_{eq} \cdot (\rho_{eq,m}/\rho_{3,c})^{0.25} = 0.044$ mm {58}

During the era of cosmic inflation the factor $k_{expansion}$ of expansion is limited as follows:

$k_{expansion} = (\boldsymbol{\rho_{D,\infty}}/\boldsymbol{\rho_{3,c}})^{1/(D+1)} \leq (\boldsymbol{\rho_{D,\infty}}/\boldsymbol{\rho_{3,c}})^{1/4}$

or $k_{expansion} \leq (0.5/0.00657)^{1/4} = 2.96$

or $N_{expansion} = \ln(k_{expansion}) \leq 1.09$ {59}

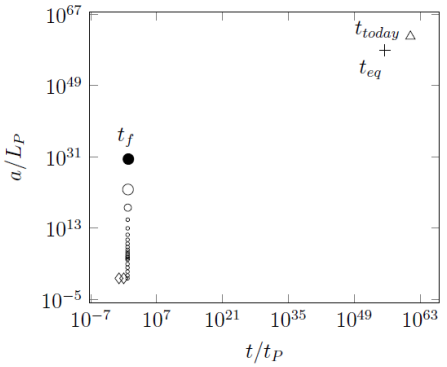

Figure 11: Radius r(t) of the current light horizon as a function of time. Circles: dimensional transitions. Diamonds: duration 6.58 t_P before D = 300 emerged (Carmesin, 2018a).

16. Enlargement by dimensional unfolding

In this lesson the students calculate the enlargement factor $Z_{unfolding}$ caused by dimensional unfolding. For it they summarize geometric properties of unfolding:

At each transition the wave functions describing the radius b of the probing mass at the higher dimension D+1 and at the lower dimension D should fit in order to obtain a high transition rate (for details see Carmesin, 2018a). As a consequence the following densities should be equal (see equation {46}):

$$\boldsymbol{\rho_{D+1}} = \boldsymbol{\rho_D} \quad \{60\}$$

Three dimensional space becomes stable at densities lower than the critical density (see figure 9):

$$\boldsymbol{\rho_{3,c}} = 0.00657 \quad \{61\}$$

At high dimension the density tends to 0.5 (see figure 10):

$$\lim_{D \to \infty} \boldsymbol{\rho_D} = 0.5 = \boldsymbol{\rho_{D,\infty}} \quad \{62\}$$

A dimensional transition is not an expansion (this is illustrated in figure 8). Thereby the dimension changes from D+1 to D. We model the volume in terms of n geometric bodies, each with an extension L_P. For simplicity we utilize n balls with the radius L_P. Other geometric bodies could be utilized similarly. The dimensional transition does neither modify the radius nor the number n as the dimensional transition merely reorganizes the connections among grains of space – this is perfectly illustrated by figure (8). So the radius of the whole system changes from r_{D+1} to r_D as follows:

$n = V_{D+1} \cdot r_{D+1}{}^{D+1} / (V_{D+1} \cdot L_P{}^{D+1}) = V_D \cdot r_D{}^D / (V_D \cdot L_P{}^D)$ {63}

We simplify by cancelling equal factors as follows:

$$n = r_{D+1}{}^{D+1}/L_P{}^{D+1} = r_D{}^D/L_P{}^D \quad \{64\}$$

$$\text{or} \quad n = \boldsymbol{r_{D+1}}{}^{\boldsymbol{D+1}} = \boldsymbol{r_D}{}^{\boldsymbol{D}} \quad \{65\}$$

When we think backwards in time, then during the era of cosmic inflation the space is folded at each dimensional transition from D to D+1 until at most two spheres are neighbors in each dimensional direction. This occurs at a corresponding dimension D_{max}. Here the currently visible space has a radius r_{Dmax} corresponding to the distance of the centers of two neighboring spheres:

$$r_{Dmax} = 2L_P \quad \text{or} \quad \boldsymbol{r_{Dmax}} = 2 \text{ and } D_{max} \approx 300 \quad \{66\}$$

The students realize that the enlargement factor $Z_{unfolding}$ or Z_u enlarges the currently visible space from its primordial extension $\boldsymbol{r_{Dmax}} = 2$ to the extension at the end of the era of cosmic inflation $\boldsymbol{r_f}$:

$$Z_u \cdot \boldsymbol{r_{Dmax}} = \boldsymbol{r_f} = 2.72 \cdot 10^{30} \quad \{67\}$$

Obviously the students solve for Z_u by utilizing equations {15} and {58}:

$Z_u = \boldsymbol{r_f}/\boldsymbol{r_{Dmax}} = r_f/r_{Dmax} = 0.044$ mm$/3.232 \cdot 10^{-35}$ m or

$Z_u = 1.36 \cdot 10^{30}$ or $N_u = \ln(Z_u) = 69.4$ {68}

The students realize that this corresponds to the observations of the CMB (Planck collaboration, 2016 or Bennett, 2013) with $55 \leq N \leq 70$ (Broy, 2016).

17. Solution of horizon problem

In this lesson the students calculate how far the light can travel in the enlarging space. For it they calculate the radius of the current light horizon as a function of time first. Here we name that radius a(t). In particular they simulate the differential equation {39} with the scaled energy in equation {50} by utilizing the Euler method and by calculating the enlargement at unfolding (see equation {65}) as follows:

$$\mathbf{a_D = a_{D+1}^{(D+1)/D}} \qquad \{69\}$$

The students calculate the duration of cosmic inflation of 3.3635 t_P. Moreover the students asked what duration a dimensional transition has. I informed them that this can be calculated and has been included in such a simulation (Carmesin, 2018a). As a result the era of cosmic inflation lasts for 22.28 t_P and the universe enlarges already for 6.58 t_P before dimension 300 is reached. Accordingly the students start the simulation at D = 300 and t = 6.58 t_P with the dynamics according to the EFLE (see equations {39} and {50}) and obtain the a(t) in figure (11).

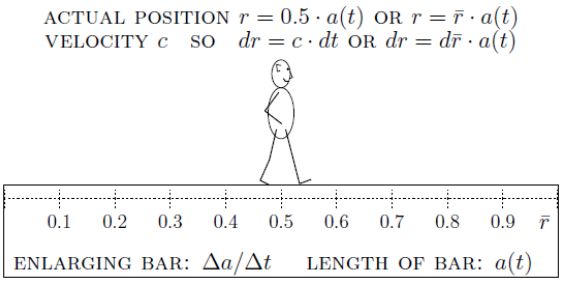

Figure 12: Radius a(t) of the current light horizon as a function of time.

The travelling of light in the enlarging space (see figure 11) is modeled by the position r(t) of a walker on an enlarging rubber bar (see figure 12). The coordinate on the bar is denoted as follows:

$$\underline{r} = r/a \qquad \{70\}$$

The students realize that the walker in figure (12) reaches the coordinate:

$$d\underline{r} = c \cdot dt/a(t) \text{ or } \underline{r} = \int_0^{tobs} c \cdot dt/a(t) \qquad \{71\}$$

The proper distance d_H that the walker reaches at a time t_{obs} of observation is the coordinate $\underline{r}$ times the length of the bar a_{obs}:

$$d_H = a_{obs} \cdot \int_0^{tobs} c \cdot dt/a(t) \qquad \{72\}$$

The students obtain $d_H = 3.291 \cdot a_{obs}$ by utilizing their simulated radius a(t) (figure 11). Causality is achieved when light can travel from one end of the CMB to the other. That amounts to the distance $d_{H,min} = 2 \cdot a_{obs} < d_H$. So the horizon problem is solved when the quantum dynamics of the transition is included.

18. Solution of the reheating problem

In this lesson the students test the alternative of an expansion instead of an unfolding (Guth, 1981 and Broy, 2016). For it they calculate the development of a primordial photon with maximal wavelength $L_P = \lambda_{prim}$. During the era of cosmic inflation that wavelength would increase at least by the factor $e^{55} = 7.7 \cdot 10^{23}$. That era ends before the time $t_{GUT} \approx 10^{-12}$ s of the grand unification at which the four fundamental forces emerged from just one fundamental force (de Boer, 2001; Bethge, 1991). Until $t_{eq} = 1.55 \cdot 10^{12}$ the wavelength would increase at least by another factor $(t_{eq}/t_{GUT})^{1/2} = 1.25 \cdot 10^{12}$. Until today the wavelength would increase by the additional factor $(t_{today}/t_{eq})^{2/3} = 4287$. Altogether the wavelength in the CMB would be at least 67 km. However, the CMB has a wavelength of 5 mm. *The students realize that the cosmic enlargement cannot completely be achieved by expansion. This is named reheating problem* (Broy, 2016). *Moreover the students realize that the present model solves the reheating problem since at least the factor e^{55} is achieved by enlargement without expansion here.*

19. Experience with teaching

The students were very interested in the topic and attended many additional meetings. It was possible to perform the method of problem solving in these lessons. Thereby we made transparent the goal, planned the solution in the plenum, solved it in groups and presented the results in the plenum. The students explained and critically tested the four models. Altogether the students actively applied the 'process related competences' of 'problem solving' and 'modeling' (Kultusministerium, 2017). Moreover these competences were especially appropriate for this teaching unit. Thereby the students efficiently developed many challenging 'content related competences' in astronomy, physics and mathematics. Some students successfully performed projects about these topics and won prizes at the Jugend forscht competition. All students appreciated that they obtained solutions based on the three fundamental constants G, c and h and the corresponding fundamental theories gravity, relativity and quantum physics.

20. Summary

Challenging and up-to-date problems about the early universe are exciting to students. A teaching unit at school has been developed and tested in a research club. The 'process related competences' of 'problem solving' and 'modeling' are especially appropriate here.

Advanced questions about the classical limit, the role of the dimension two or about the relation to other approaches in the field are elaborated in detail in Carmesin (2018d). Several students are interested to work out a well-arranged problem in this context and four such projects are currently in progress.

Published in PhysDid B (2018).

21. Literatur

Ballentine, Leslie (1998): Quantum Mechanics. London and Singapore: World Scientific Publishing.

Bennett, Charles L. and others (2013): Nine-year Wilkinson microwave anisotropy probe (WMAP) Observations: final maps and results. The Astrophysical Journal Supplement Series. 208. 1-54.

Bethge, Klaus und Schröder, Ulrich (1991): Elementarteilchen und ihre Wechselwirkungen. 2. Aufl., Darmstadt: Wissenschaftliche Buchgesellschaft.

Boer, de, Wim (2001): Grand Unified Theories and Supersymmetry in Particle Physics and Cosmology. arxiv, hep-ph/9402266v5, 1-107.

Bojowald, Martin (2001): Absence of Singularity in Loop Quantum Gravity. Phys. Rev. Lett. 86, 5227-5230.

Broy, Benedict Johannes (2016): Inflation and effective Shift Symmetries. Hamburg: Universität Hamburg. Thesis.

Carmesin, Hans-Otto (2006): Entdeckungen im Physikunterricht durch Beobachtungen des Himmels. Tagungs-CD Fachdidaktik Physik, ISBN 978-386541-190-7. Nordmeier, Volker and Oberländer, Arne (Editors). Berlin: Deutsche Physikalische Gesellschaft.

Carmesin, Hans-Otto (2012): Schüler beobachten den Urknall mit einem C11 Teleskop. PhyDid B, Internetzeitschrift, ISSN 2191-379X.

Carmesin, Hans-Otto and Carmesin, Ellen (2014): How Old is the Universe? PhyDid B, ISSN 2191-379X.

Carmesin, Hans-Otto (2017): Vom Big Bang bis heute mit Gravitation – Model for the Dynamics of Space. Berlin: Verlag Dr. Köster.

Carmesin, Hans-Otto (May 2018a): Entstehung dunkler Materie durch Gravitation - Model for the Dynamics of Space and the Emergence of Dark Matter. Berlin: Verlag Dr. Köster.

Carmesin, Hans-Otto Carmesin and Carmesin, Matthias (2018b): Quantum Gravity Model for Cosmic Inflation. To be publ.

Carmesin, Hans-Otto (July 2018c): Entstehung dunkler Energie durch Quantengravitation - Universal Model for the Dynamics of Space, Dark Matter and Dark Energy. Berlin: Verlag Dr. Köster.

Carmesin, Hans-Otto (2018d): Entstehung der Raumzeit durch elementare Quantengravitation - Universal Model for the Emergence of Space, Dark Matter, Vacuum Energy and Space-Time. Berlin: Verlag Dr. Köster, to be published.

Chandrasekhar, Subrahmanyan (1931): The maximum mass of ideal white dwarfs. Astrophysical Journal, 74, 81-82.

Friedmann, Alexander (1922): Über die Krümmung des Raumes. Z. f. Physik, 10, 377-386.

Gauss, Carl Friedrich (1813): Theoria attractionis corporum sphaeroidicorum ellipticorum homogeneorum – methoda novo tractata. Societ. Reg. Scient. Tradita. 1-24.

Guth, Alan (1981): Inflationary Universe: A possible to the horizon and flatness problem. Phys. Rev. D 23, 347-356.

Hattie, John (2009): Visible Learning. London: Routledge.

Helmcke, Ben Joshua; Carmesin, Hans-Otto; Sprenger, Lennert und Brüning, Paul (2018): Three methods for the observation of the Big Bang with our school telescope. PhyDid B.

Hubble, Edwin (1929): A relation between distance and radial velocity among extra-galactic nebulae. Proc. of National Acad. of Sciences, 168-173.

Kiefer, Claus and Sandhöfer, Barbara (2008): Quantum Cosmology. Beyond the Big Bang. Vaas, Rüdiger (Herausgeber). Berlin: Springer, 1-29.

Kircher, Ernst and Girwidz, Raimund and Häußler, Peter (2001): Physikdidaktik. Berlin: Springer. 2. Auflage.

Kultusministerium, Niedersächsisches (2017): Kerncurriculum für das Gymnasium - gymnasiale Oberstufe, die Gesamtschule - gymnasiale Oberstufe, das Fachgymnasium, das Abendgymnasium, das Kolleg, Chemie, Niedersachsen. Hannover: Niedersächsisches Kultusministerium.

Lemaitre, Georges (1927): Un Univers homogene de masse constante et de rayon croissant rendant compte de la vitesse radiale des nebuleuses extra-galactiques. Annales de la Societe Scientifique de Bruxelles. A47, 49-59.

Planck, Max (1899): Über irreversible Strahlungsvorgänge. Sitzungsberichte der Königlich Preußischen Akademie der Wissenschaften zu Berlin. Berlin: Verlag der Kgl. Preuß. Akad. der Wiss., 440-480.

Planck Collaboration (2016): Planck 2015 Results: Cosmological Parameters. Astronomy and Astrophysics. 594, 1-63.

Popper, Karl (1974): Objektive Erkenntnis. 2. Auflage. Hamburg: Hoffmann und Campe.

Sexl, Roman und Sexl, Hannelore (1975): Weiße Zwerge – schwarze Löcher. Reinbek bei Hamburg: Rowohlt.

Sprenger, Lennert und Carmesin, Hans-Otto (2018): A Computer Simulation of Cosmic Inflation. PhyDid B.

Unsöld, Albrecht and Baschek, Bodo (1999): Der neue Kosmos. Berlin: Springer. 6. Auflage.

Wirtz, Carl (1922): Radialbewegung der Gasnebel. Astronomische Nachrichten, 215, 281-286.